BMC Medical Genomics

RESEARCH

Open Access

Association of metabolic dysregulation with treatment response in rectal cancer patients undergoing chemoradiotherapy

Qiliang Peng[1,2,3†], Yi Shen[4†], Yingying Xu[1,2†], Zhengyang Feng[3,5†], Yao Xu[6], Yong Wang[1,2], Li Zou[1,2], Yaqun Zhu[1,2*] and Yuntian Shen[1,2*]

Abstract

Background This study aimed to explore the metabolic changes during neoadjuvant chemoradiotherapy (NCRT) in patients with locally advanced rectal cancer (LARC) by serum metabolomics analysis, and to provide new biomarkers for individualized treatment and efficacy prediction.

Methods Serum samples from 20 patients with LARC before, during and after NCRT were collected for metabolomic analysis. The metabolites in the serum samples were analyzed qualitatively and quantitatively using gas chromatography-mass spectrometry (GC-MS). Meanwhile, the differences in metabolic profiles at different time points were compared and significantly changed metabolites were screened.

Results The metabolic profiles of patients were significantly altered at different time points of NCRT. Through metabolomic analysis, we identified metabolites that were significantly altered during NCRT and revealed alterations in the associated metabolic pathways. The predictive power of pre-radiotherapy isocitric acid and pro-radiotherapy 3-hydroxy-3-(4′-hydroxy-3′-methoxyphenyl) propionic acid in distinguishing patients sensitive and non-sensitive to NCRT was markedly high, with AUC values of 0.875 and 0.75, respectively. Additional analysis indicated that a combined panel of serum metabolites yielded even higher AUC values, thereby enhancing the accuracy of predicting the efficacy of neoadjuvant NCRT.

Conclusion This study revealed metabolic changes and corresponding alterations in metabolic pathways during NCRT in patients with LARC by serum metabolomic analysis. The metabolic disorders may be associated with poor outcomes in patients treated with NCRT for rectal cancer, providing new biomarkers for individualized treatment and prognostic assessment. Further studies and validation will help to gain insight into the mechanism of these metabolic changes and provide more basis for clinical application.

Keywords Rectal cancer, Neoadjuvant chemoradiotherapy, Metabolic disorders, Biomarker

†Qiliang Peng, Yi Shen, Yingying Xu and Zhengyang Feng contributed equally to this work.

*Correspondence:
Yaqun Zhu
szzhuyaqun@sina.com
Yuntian Shen
shenyuntian2001@sina.com

Full list of author information is available at the end of the article

Introduction

Rectal cancer is a prevalent malignancy with high incidence and mortality rates worldwide [1]. In cases of locally advanced rectal cancer (LARC), the tumor has typically infiltrated the deeper layers of the intestinal wall without distant lymph node or organ metastasis. This stage presents significant therapeutic challenges, as the tumor size is often substantial, surgical resection is more complex, and the risk of lymph node metastasis remains a concern [2]. The current standard of care for LARC involves neoadjuvant chemoradiotherapy (NCRT) followed by total mesorectal excision [3]. However, patient responses to NCRT are highly heterogeneous. While approximately 10-30% of patients achieve a pathological complete response and 40-45% exhibit partial tumor regression, 20-30% of patients show little to no response to NCRT [4]. This variability underscores the need for reliable biomarkers to predict treatment response early in the course of therapy. Identifying such biomarkers would enable clinicians to tailor preoperative treatments based on individual sensitivity to NCRT, ultimately improving patient outcomes and advancing personalized treatment strategies for LARC.

In recent years, metabolomics has emerged as a powerful tool in cancer research, offering significant advancements in understanding tumor biology and treatment response [5]. As a comprehensive approach to profiling the chemical composition and metabolic activities of biological systems, metabolomics provides unique insights into tumor initiation, progression, and therapeutic outcomes. It has been widely applied in cancer biomarker research, including early detection, diagnosis, prognosis prediction, and treatment efficacy evaluation [6]. Previous studies have demonstrated that metabolism-related biomarkers may correlate with differential responses to NCRT in rectal cancer [7]. Additionally, evidence suggests that serum metabolites can distinguish between NCRT-sensitive and non-sensitive patients, offering potential for predicting treatment efficacy [8, 9]. These findings highlight the potential of metabolic biomarkers as key factors influencing rectal cancer radiosensitivity. However, the underlying mechanisms remain poorly understood and warrant further investigation to unlock their full clinical potential.

In recent years, gas chromatography-mass spectrometry (GC-MS) has emerged as a powerful analytical tool in tumor biomarker research, combining the separation capabilities of gas chromatography with the sensitive detection of mass spectrometry. This enables efficient and highly accurate qualitative and quantitative analysis of compounds in complex biological samples [10]. In the field of cancer research, GC-MS has been instrumental in identifying potential tumor markers-molecules specifically associated with tumorigenesis, progression, and metastasis [11]. By analyzing metabolites in tumor tissues, blood, urine, and other biofluids, GC-MS can uncover characteristic metabolic signatures linked to cancer, providing a foundation for early diagnosis and targeted treatment strategies [12]. Furthermore, GC-MS plays a critical role in monitoring drug metabolism during cancer therapy. By tracking changes in the concentration of drug metabolites in patients, it enables the evaluation of treatment efficacy and side effects, thereby supporting personalized therapeutic approaches [13]. As GC-MS technology continues to advance, its applications in tumor biomarker research are expected to expand further, offering new opportunities for improving cancer diagnosis, treatment, and patient outcomes.

This study utilized GC-MS to investigate dynamic changes in serum metabolites during NCRT in patients with LARC. Our primary objective was to identify differential metabolites before and after NCRT, as well as between patients with varying sensitivity to treatment. By analyzing these metabolic changes, we aimed to uncover dysregulated metabolic pathways and identify potential biomarkers capable of distinguishing between NCRT-sensitive and non-sensitive patients. These findings could provide a valuable foundation for the early prediction of treatment response and facilitate timely therapeutic interventions, ultimately improving outcomes for rectal cancer patients undergoing NCRT.

Materials and methods

Case selection

The study cohort comprised 20 individuals with locally advanced rectal cancer who underwent neoadjuvant chemoradiotherapy (NCRT) at the Second Affiliated Hospital of Soochow University between January and December 2022. Inclusion criteria were as follows: (1) Pathologically confirmed rectal adenocarcinoma with no prior treatment history. (2) Classified as stage III based on the American Joint Committee on Cancer (AJCC) 8th edition criteria. (3) Karnofsky Performance Status (KPS) score ≥ 70, indicating adequate general health. (4) Primary tumor within 10 cm of the anal verge. Patients were excluded if they met any of the following: (1) History of pelvic radiotherapy or other malignancies; (2) Severe comorbidities precluding NCRT completion; (3) Incomplete baseline imaging data. Ethical approval for this study was granted by the Ethics Committee of the Second Affiliated Hospital of Soochow University.

Treatment situation

The therapeutic regimen for this cohort of patients adheres to the experimental protocol outlined in the multicenter clinical investigation known as the CinClare study, which is spearheaded by the Fudan University Shanghai Cancer Center [14]. Every patient in this study

embarked on a long-course concurrent chemoradiotherapy regimen, utilizing 6 MV X-ray intensity-modulated radiotherapy (IMRT) technology. The treatment fields encompassed the primary tumor lesion, the rectal mesorectal region, the presacral area, the iliac lymphatic drainage region, and the common iliac lymphatic drainage zone. The clinical target volume was expanded by 0.5 to 1.0 cm to establish the planning target volume. The radiotherapy dose administered to all patients was 50 Gy, delivered in 25 fractions, with treatment administered from Monday to Friday for a cumulative period of 5 weeks. Concurrent chemotherapy involved the use of either single-agent capecitabine or a combination of capecitabine with irinotecan. For the interval chemotherapy phase, the XELOX or XELIRI chemotherapy regimens were employed. Surgical intervention was scheduled 6–8 weeks following the completion of concurrent chemoradiotherapy, with the specific surgical approach-such as the Miles, Dixon, or Hartmann procedure-determined by the operating surgeon.

Patient grouping

The postoperative pathological assessment for the entire cohort was conducted utilizing the tumor regression grading (TRG) system. This system encompasses four distinct categories: TRG 0, indicative of complete tumor regression; TRG 1, denoting near-complete regression; TRG 2, indicating partial regression; and TRG 3, which characterizes minimal to no regression of the tumor [15]. For the purposes of this investigation, we categorized patients with a TRG of 0 or 1 as radiotherapy-sensitive, whereas those with a TRG of 2 or 3 were classified as radiotherapy-insensitive.

Serum collection and preparation

Blood serum specimens were procured from all participants at three distinct time points: prior to radiotherapy (RB, collected within three days leading up to the initiation of radiotherapy), mid-radiotherapy (RD, on the 15th day of radiation treatment), and following radiotherapy (RA, gathered within three days after the conclusion of radiotherapy). These samples were transferred into serum-specific tubes. Subsequently, the tubes were kept at ambient temperature for 15–30 min to facilitate blood clotting. The clots were subsequently removed by centrifugation at 4 °C, at a speed of 1000 g, for a duration of 10 min. The cleared supernatant was then carefully aspirated and stored at -80 °C pending further sample processing. For analysis, 150 ul of the thawed serum was transferred into 1.5-mL Eppendorf tubes, to which 10 ul of an internal standard (L-2-chlorophenylalanine at a concentration of 0.3 mg/mL) was added. Following this, 450 ul of a protein precipitating mixture of methanol and acetonitrile was introduced. The mixture was subjected to ice-water bath sonication for 10 min, followed by a 30-minute incubation at -20 °C, and another round of centrifugation. The resulting supernatant was transferred into a glass derivatization vial, and the sample was concentrated using a freeze-concentration centrifugal dryer. The next step involved the addition of 80 ul of a pyridine methoxylamine hydrochloride solution (at a concentration of 15 mg/mL), followed by vortexing and shaking for 2 min. The oxidation reaction was then conducted at 37 °C for 90 min in a shaking incubator. Post-reaction, 50 ul of BSTFA (containing 1% TMCS) derivatization reagent and 20 ul of n-hexane were added to the samples, along with 10 ul of the internal standard. The samples were vortexed and shaken for an additional 2 min before being placed in a 70 °C incubator for 60 min. After the derivatization process, the samples were allowed to cool to room temperature for 30 min, at which point they were ready for GC-MS metabolomics analysis.

GC-MS analysis

Metabolites were fractionated utilizing a DB-5MS capillary column (manufactured by Agilent J&W Scientific, Folsom, CA, USA). The analytical process employed high-purity helium gas (with a minimum purity of 99.999%) as the carrier, maintained at a flow rate of 1.0 mL/min. The injection port was set to a temperature of 260 °C. The sample injection was performed in a 1 ul volume without split injection, and a solvent delay of 5 min was implemented to precede data acquisition. For effective metabolite separation, the oven temperature of the gas chromatograph was programmed to rise from an initial temperature of 60 °C to a final temperature of 305 °C. The inlet and ion source temperatures were both maintained at 230 °C. Electron ionization (EI) was the ionization method of choice, operated at an ionization energy of 70 eV. The mass spectrometer was operated in full scan mode, covering a mass-to-charge ratio (m/z) range from 50 to 500.

Metabolite identification

The raw GC/MS data files, in D format, were initially transformed into an analysis base file using the Analysis Base File Converter software to facilitate swift data access. Subsequently, these files were imported into the MS-DIAL software suite for an extensive series of preprocessing steps. This workflow encompassed peak detection, peak identification, MS2Dec deconvolution, spectral characterization, peak alignment, data filtering, and the interpolation of missing values to ensure comprehensive data integrity [16]. The precursor ion peaks were meticulously pinpointed through the analysis of two contiguous data axes. Utilizing the MS2Dec algorithm, "model peaks" were diligently extracted from the chromatograms, effectively eliminating background noise

and refining the molecular mass based on retention time. Metabolite identification was achieved by cross-referencing with the Untarget database for GC-MS, developed by Lumingbio using a suite of chemical standards. For the metabolites that remained unidentified, a thorough screening was conducted against a comprehensive NIST mass spectral library [17].

Statistical analysis

The relative concentrations of non-target metabolites were standardized against the abundance of the internal standard and the total ion counts [18]. Principal component analysis (PCA) was initially employed to survey the overall distribution across the samples and to gauge the stability of the entire analytical process. Subsequently, partial least squares analysis (PLS-DA) and orthogonal partial least squares analysis (OPLS-DA) were implemented to discern the overarching discrepancies in metabolic profiles among the various groups [19]. Furthermore, variable importance in projection (VIP) values were calculated using OPLS-DA analysis to quantify the strength of influence and explanatory power of the expression pattern of each metabolite on the categorical discrimination of each group of samples. This allowed us to identify biologically significant differential metabolites [20]. An independent samples t-test was subsequently employed to corroborate the statistical significance of the differential metabolites between the groups. The screening criteria were set at VIP values > 1 for the first principal component of the OPLS-DA model and P values < 0.05 for the t-test. Z-Score plots were then generated to normalize the data and enhance data comparability. By employing the R package Mfuzz, which utilizes fuzzy clustering principles, each metabolite was assigned to multiple clusters. By calculating the membership value of each metabolite within each cluster, the degree of its association with a particular cluster was visually represented [21]. Pearson's correlation coefficient was employed for correlation analysis to examine the degree of association between the differential metabolites. The KEGG database was then utilized to analyze the downstream metabolic pathways that were potentially enriched by the differential metabolites [22]. Statistical significance was established at $P < 0.05$ for metabolic pathways. Finally, a machine learning algorithm, incorporating random forests and ROC curves, was employed to identify key metabolites and to assess their predictive capacity for radiotherapy sensitivity [23, 24]. To assess the significance of differential metabolites, we utilized the metrics of mean decrease accuracy and mean decrease Gini [25].

Table 1 The baseline characteristics of included patients

Variable	Total	NCRT sensitive	NCRT non-sensitive
Patient number	20	6	12
Age, year	67.5 ± 10.4	67.5 ± 10.9	67.5 ± 10.2
Male, n (%)	15 (75%)	3 (50%)	10 (83.3%)
Tumor distance	5.3 ± 1.5	5.8 ± 1.9	5.1 ± 1.4
Tumor length	5.1 ± 1.3	4.5 ± 1.0	5.2 ± 1.1
Clinical T stage			
T3	13	4	8
T4	7	2	4
Clinical N stage			
N1	6	2	4
N2	14	4	8
TRG			
0	4	4	-
1	2	2	-
2	10	-	10
3	2	-	2

Results

Study population and characteristics

The study cohort comprised a total of 20 patients, and a detailed breakdown of their demographics is provided in Table 1. Of this group, two individuals did not receive surgical intervention at our institution, precluding the assessment of treatment efficacy through postoperative pathological evaluation. The remaining 18 patients were categorized into two distinct groups based on their response to therapy, consisting of 6 cases exhibiting sensitivity and 12 cases demonstrating non-sensitivity.

Quality control

Quality control (QC) samples were employed to prime the "chromatography-mass spectrometry" system before the commencement of sample analyses and to monitor the consistency of the mass spectrometry system throughout the testing process. The total ion chromatogram derived from the QC samples is depicted in Fig. 1A. The data revealed that the peak response intensities and retention times exhibited a high degree of overlap, suggesting minimal instrumental variability across the entire experimental procedure. Unsupervised PCA demonstrated that the QC samples and experimental samples formed distinct, cohesive clusters, signifying the robust stability and reproducibility of the experimental protocol (Fig. 1B). The intensity distribution of metabolites (Fig. 1C) and the hierarchical clustering of all metabolites (Fig. 1D) further validated the excellent stability achieved in this study.

Changes in serum metabolites during NCRT in the entire patient group

To investigate the impact of radiotherapy on the serum metabolome of rectal cancer patients, an untargeted metabolomics strategy was employed to analyze serum samples from 20 patients at three critical junctures:

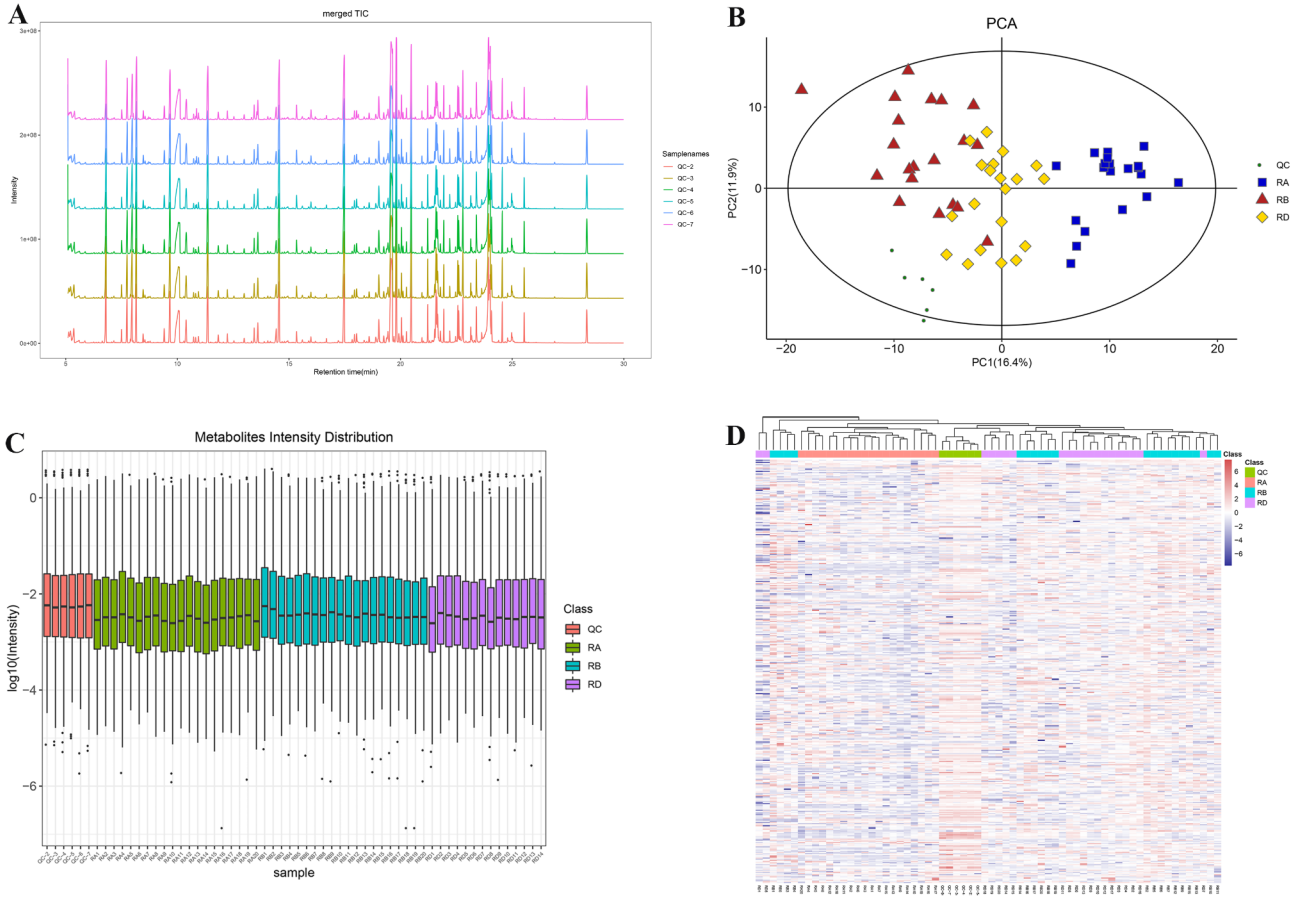

Fig. 1 Quality control of all the samples. **(A)** Total ion chromatogram of quality control samples; **(B)** Principle component analysis of all the samples; **(C)** Metabolites intensity distribution; **(D)** Hierarchical clustering of all the metabolites

before, during, and after radiotherapy. At each of these timepoints (RB, RD, and RA), PCA, PLS-DA, and OPLS-DA all clearly demarcated the samples, signifying substantial alterations in serum metabolites throughout NCRT (Fig. 2A-I). To ensure the reliability and stability of the model, 200 permutation tests were performed, with R2 and Q2 values confirming the model's viability for subsequent optimization analyses (Fig. 2J-L). By cross-referencing with the EMDB database and filtering for endogenous differential metabolites with VIP scores greater than 1 and p-values less than 0.05, a set of potential differential metabolites was identified. As depicted in the volcano plots (Fig. 3A-C), there were 75, 101, and 100 differential metabolites in the RD vs. RB, RA vs. RD, and RA vs. RB comparisons, respectively. Heatmaps were also generated to visualize these differences (Fig. 3D-F). A total of 31 metabolites were found to be commonly altered across these comparisons, including nicotinic acid, N-acetylglutamate, uracil, pyrophosphate, and L-2-hydroxyglutaric acid. Further analysis revealed intrinsic associations among these differential metabolites (Fig. 3G-I). Additionally, a greater overlap of differential metabolites was observed between the RA and RD groups and between the RA and RB groups, totaling 75 metabolites, with notable changes observed in several lipid metabolites such as arachidonic acid. Time series analysis, a widely adopted technique in metabolomics for uncovering trends in metabolite levels across different time points, was utilized to explore the dynamic nature of metabolic pathways and to pinpoint time-dependent biological processes. Consequently, eight significant clusters of serum metabolites with pronounced time trends were delineated (Fig. 4). These clusters similarly encompassed multiple key lipid metabolites.

Metabolic pathways during NCRT in the entire patient group

To delve into the alterations of serum metabolic pathways instigated by radiotherapy in rectal cancer, the identified differential metabolites were analyzed through metabolic pathway enrichment. The findings revealed that the 75 differential metabolites between the RD and RA groups were significantly associated with 27 metabolic pathways, encompassing central carbon metabolism in cancer, oxidative phosphorylation, tyrosine metabolism, arginine biosynthesis, lysine degradation,

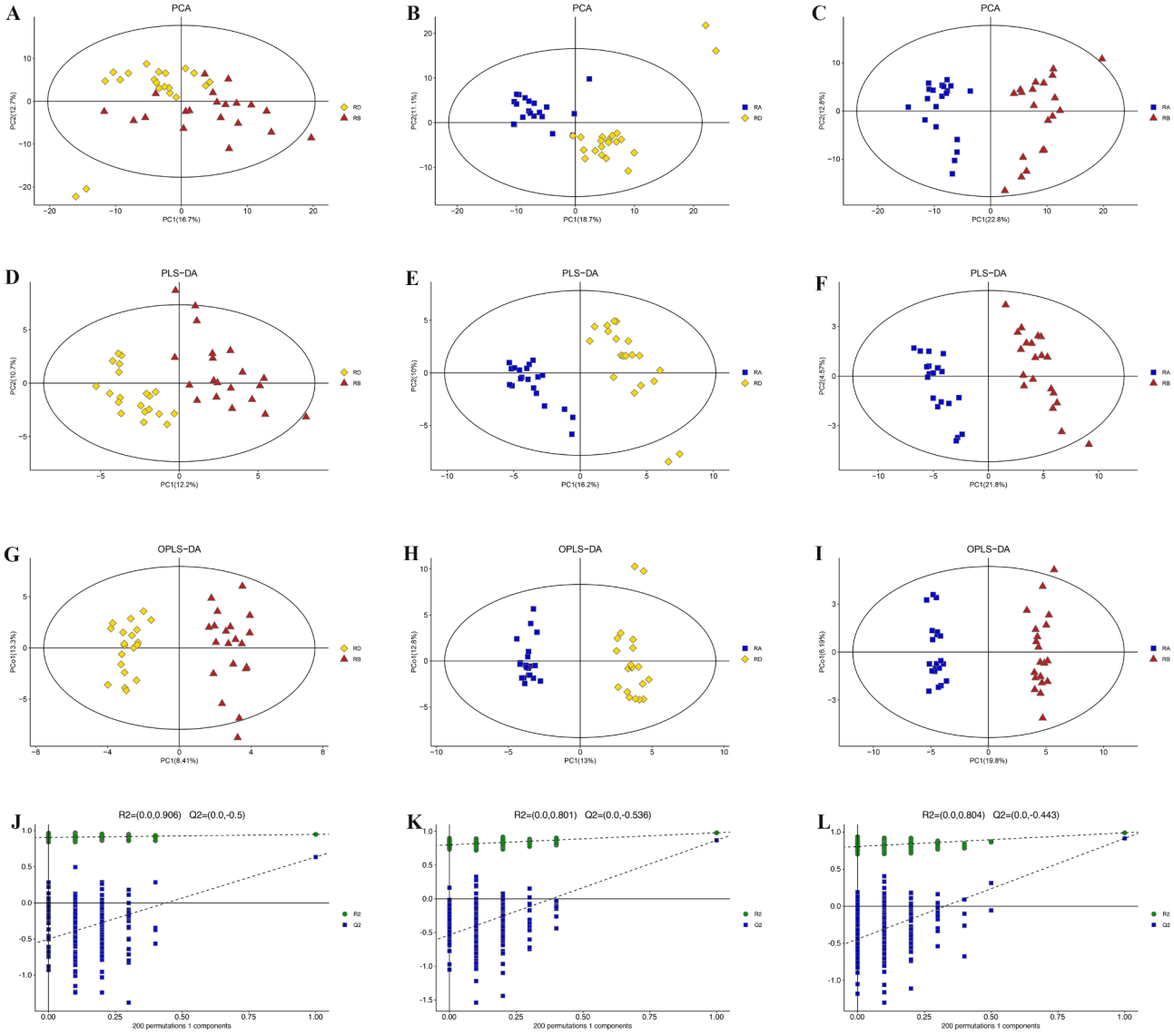

Fig. 2 Multivariate statistical analysis of the overall differences among different timepoints groups during NCRT. **(A)** PCA score plots of the overall differences between RD and RB groups. **(B)** PCA score plots of the overall differences between RA and RD groups. **(C)** PCA score plots of the overall differences between RA and RB groups. **(D)** PLS-DA score plots of the overall differences between RD and RB groups. **(E)** PLS-DA score plots of the overall differences between RA and RD groups. **(F)** PLS-DA score plots of the overall differences between RA and RB groups. **(G)** OPLS-DA score plots of the overall differences between RD and RB groups. **(H)** OPLS-DA score plots of the overall differences between RA and RD groups. **(I)** OPLS-DA score plots of the overall differences between RA and RD groups. **(J)** Permutation chart of the overall differences between RD and RB groups. **(K)** Permutation chart of the overall differences between RA and RD groups. **(L)** Permutation chart of the overall differences between RA and RB groups

the mTOR signaling pathway, and the PI3K-Akt signaling pathway (Fig. 5A, B). The analysis further disclosed that the 101 differential metabolites between the RA and RD groups were prominently linked to 11 metabolic pathways, which included the biosynthesis of unsaturated fatty acids, pyrimidine metabolism, valine, leucine, and isoleucine biosynthesis, ferroptosis, central carbon metabolism in cancer, galactose metabolism, lysine degradation, and arginine biosynthesis, as well as ABC transporters (Fig. 5C, D). Moreover, the study indicated that the 100 differential metabolites between the RA and RB groups were substantially correlated with 20 metabolic pathways, primarily involving key pathways such as lysine degradation, alanine, aspartate, and glutamate metabolism, central carbon metabolism in cancer, oxidative phosphorylation, ferroptosis, pyrimidine metabolism, pyruvate metabolism, and the regulation of lipolysis in adipocytes (Fig. 5E, F). A convergence of five metabolic pathways was observed across these groups, including central carbon metabolism in cancer, renal cell carcinoma, arginine biosynthesis, lysine degradation, and pyrimidine metabolism.

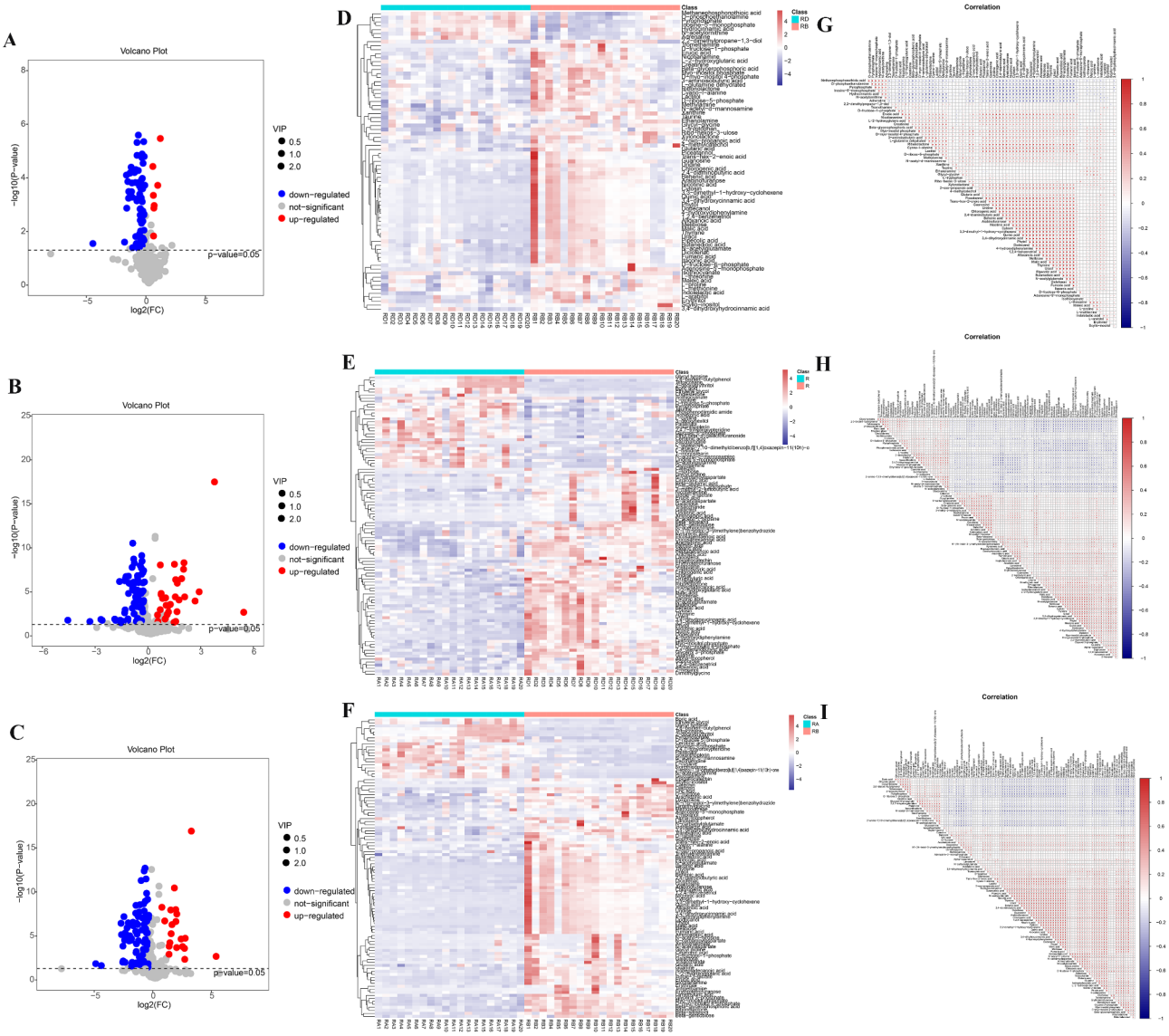

Fig. 3 Key metabolites identified across different timepoints during NCRT. (**A**-**C**) Volcano plots illustrating differentially expressed metabolites: RD vs. RB (**A**), RA vs. RD (**B**), and RA vs. RB (**C**). (**D**-**F**) Heatmaps visualizing the expression patterns of key metabolites: RD vs. RB (**D**), RA vs. RD (**E**), and RA vs. RB (**F**). (**G**-**I**) Correlation analyses of key metabolites: RD vs. RB (**G**), RA vs. RD (**H**), and RA vs. RB (**I**)

Changes in serum metabolites during NCRT in different sensitivity groups

Serum samples collected before and after radiotherapy were categorized into four distinct groups: RB-S (sensitive group pre-radiotherapy), RB-NS (non-sensitive group pre-radiotherapy), RA-S (sensitive group post-radiotherapy), and RA-NS (non-sensitive group post-radiotherapy). We conducted an in-depth examination of the metabolic shifts across the four comparative groups, which included RA-S versus RB-S, RA-NS versus RB-NS, RB-S versus RB-NS, and RA-S versus RA-NS. The PLS-DA and OPLS-DA score plots, supplemented by permutation tests, demonstrated a clear demarcation between the samples of varying sensitivity groups, indicating the stability of the models (Fig. 6). The impact of radiotherapy on metabolite alterations within different sensitivity groups was initially investigated. In the sensitive group, a total of 88 metabolites exhibited significant changes following radiotherapy (Fig. 7A, B), while the non-sensitive group saw 89 metabolites with significant post-radiotherapy changes (Fig. 7D, E). Z-Score plots were generated to normalize the data, enhancing its comparability (Fig. 7C and F). These metabolites exhibited a robust intrinsic linkage among themselves (Fig. 7G-J).

Subsequently, the contrast in pre-radiotherapy serum metabolites between the sensitive and non-sensitive patient groups was scrutinized (Fig. 8A). The analysis revealed 23 metabolites that exhibited significant

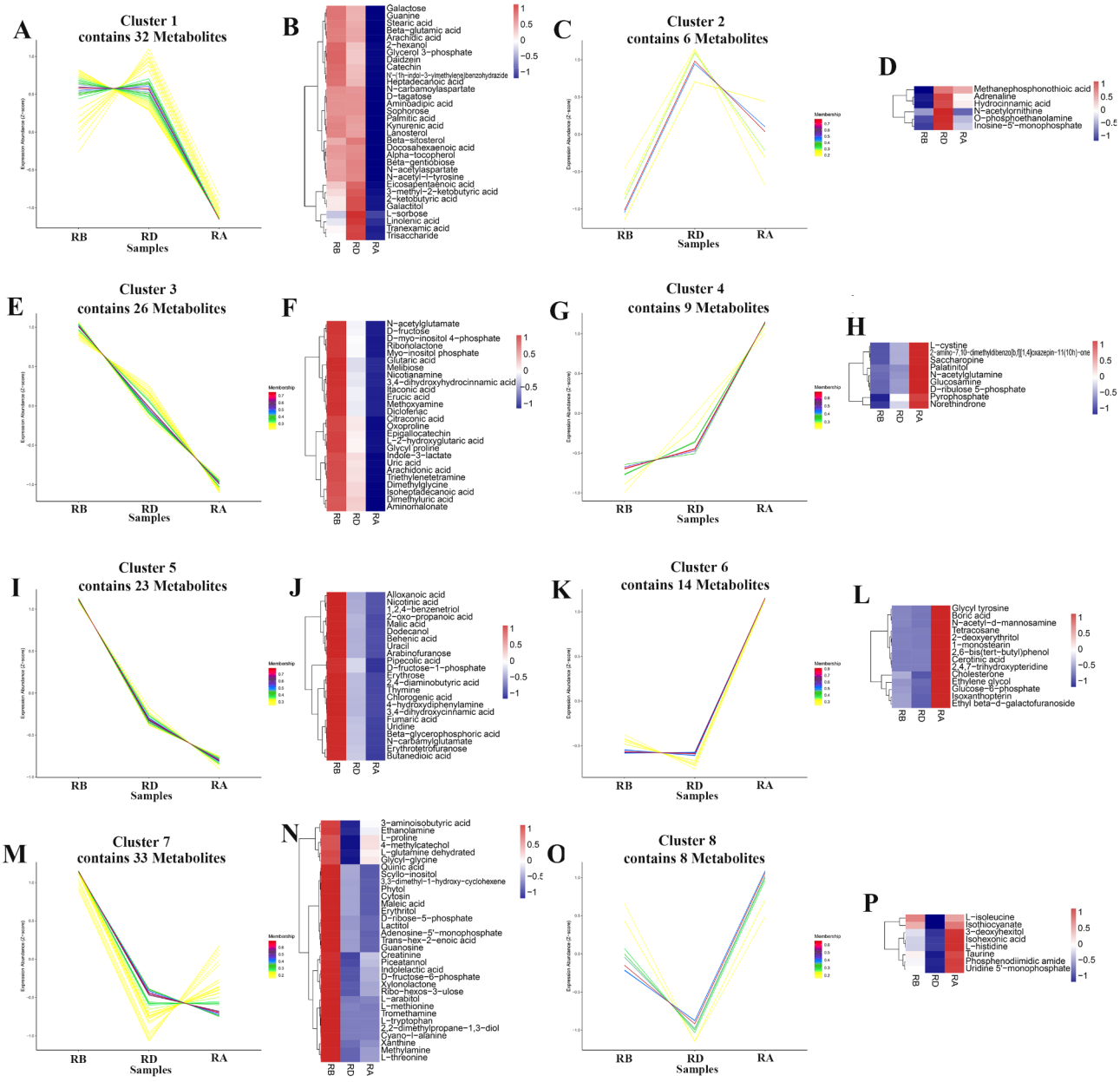

Fig. 4 Significant time trend clusters of serum metabolites during NCRT. **(A-B)** Time trend and heatmap of Cluster 1, comprising 32 metabolites. **(C-D)** Time trend and heatmap of Cluster 2, comprising 6 metabolites. **(E-F)** Time trend and heatmap of Cluster 3, comprising 26 metabolites. **(G-H)** Time trend and heatmap of Cluster 4, comprising 9 metabolites. **(I-J)** Time trend and heatmap of Cluster 5, comprising 23 metabolites. **(K-L)** Time trend and heatmap of Cluster 6, comprising 14 metabolites. **(M-N)** Time trend and heatmap of Cluster 7, comprising 33 metabolites. **(O-P)** Time trend and heatmap of Cluster 8, comprising 8 metabolites

differences between the RB-S and RB-NS groups, including L-isoleucine, formononetin, and glucosamine (Fig. 8C). This suggests that serum metabolites may contribute to the early progression of rectal cancer, thereby influencing radiosensitivity. Moreover, the comparison of serum metabolites in the sensitive and non-sensitive groups post-radiotherapy was conducted (RA-S versus RA-NS, as shown in Fig. 8B). The investigation yielded seven metabolites with significant differences between the two post-radiotherapy patient groups, including L-isoleucine, 1-monostearin, and 2-ketobutyric acid (Fig. 8D). Z-scores were utilized for data standardization (Fig. 8E, F), and a notable correlation among metabolites was identified (Fig. 8G, H). By identifying the intersection of these differences, L-isoleucine was found to exhibit significant variations in both the sensitive and non-sensitive groups before and after radiotherapy, suggesting

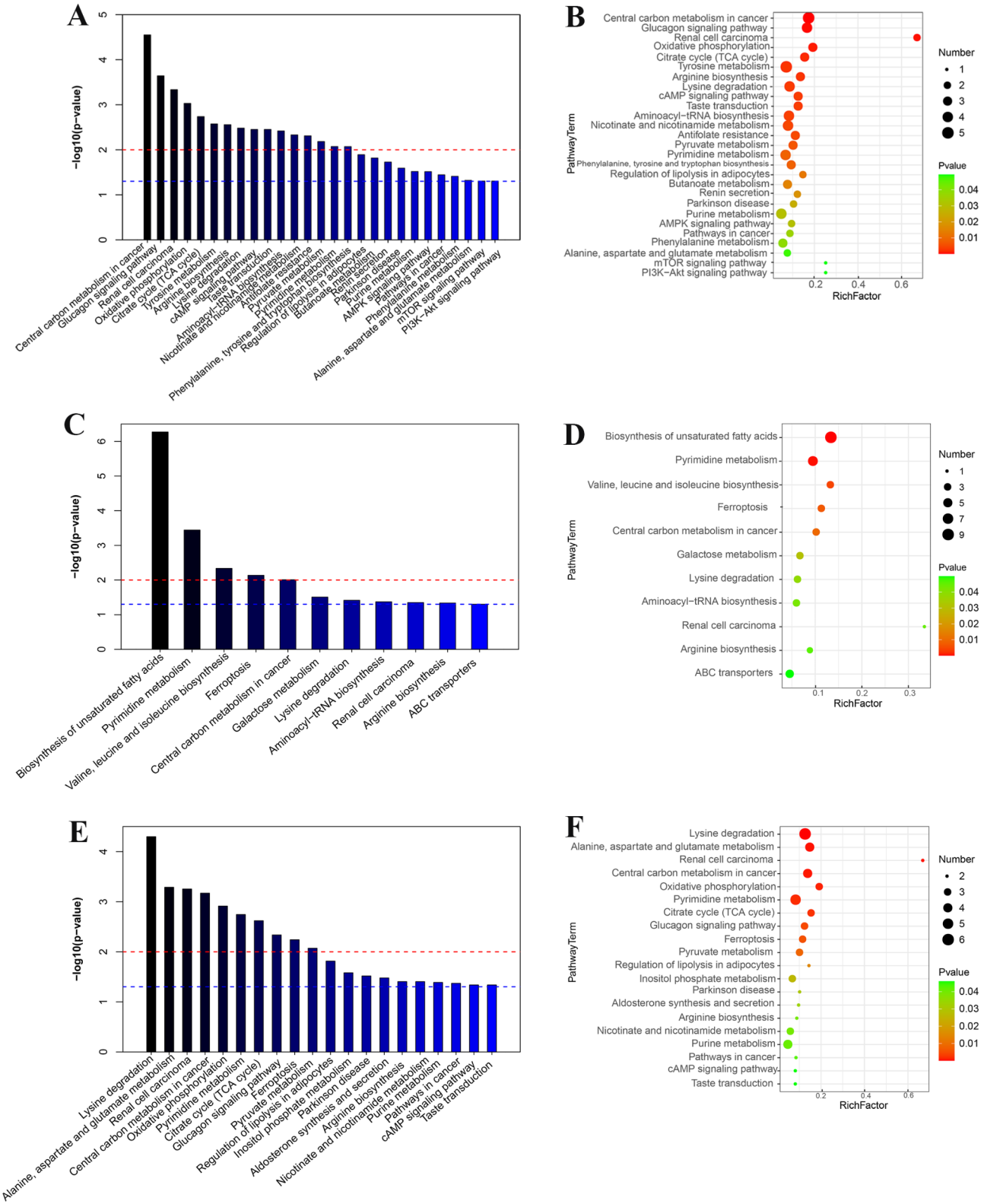

Fig. 5 Significantly enriched metabolic pathways across different timepoints during NCRT. **(A-B)** Bar charts and bubble plots illustrating significantly enriched metabolic pathways between RD and RB. **(C-D)** Bar charts and bubble plots illustrating significantly enriched metabolic pathways between RA and RD. **(E-F)** Bar charts and bubble plots illustrating significantly enriched metabolic pathways between RA and RB

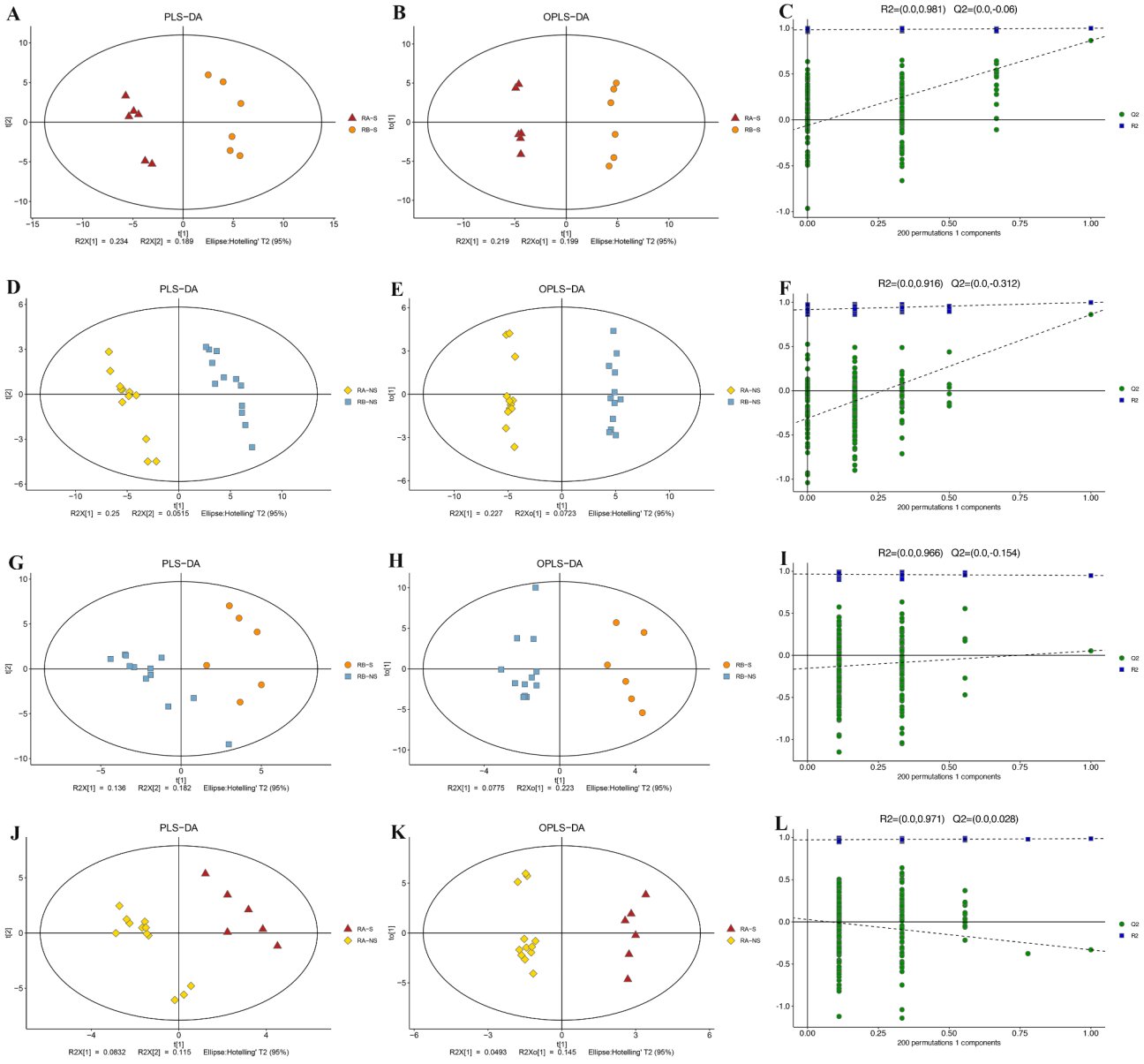

Fig. 6 Multivariate statistical analysis of metabolic differences between sensitivity groups during NCRT. **(A)** PLS-DA score plots comparing RA-S and RB-S groups. **(B)** OPLS-DA score plots comparing RA-S and RB-S groups. **(C)** Permutation test results for RA-S and RB-S groups. **(D)** PLS-DA score plots comparing RA-NS and RB-NS groups. **(E)** OPLS-DA score plots comparing RA-NS and RB-NS groups. **(F)** Permutation test results for RA-NS and RB-NS groups. **(G)** PLS-DA score plots comparing RB-S and RB-NS groups. **(H)** OPLS-DA score plots comparing RB-S and RB-NS groups. **(I)** Permutation test results for RB-S and RB-NS groups. **(J)** PLS-DA score plots comparing RA-S and RA-NS groups. **(K)** OPLS-DA score plots comparing RA-S and RA-NS groups. **(L)** Permutation test results for RA-S and RA-NS groups

its potential involvement in the response to rectal cancer radiotherapy.

Metabolic pathways during NCRT in different sensitivity groups

To elucidate the metabolic pathways and the interrelationships among the metabolites associated with the differential metabolites in patients displaying varied radiosensitivity before and after radiotherapy, pathway enrichment analysis was conducted on the differential metabolites across the four comparative groups: RA-S versus RB-S, RA-NS versus RB-NS, RB-S versus RB-NS, and RA-S versus RA-NS. Post-radiotherapy, a total of 21 metabolic pathways in the sensitive group displayed significant alterations (Fig. 9A), while the non-sensitive group exhibited significant changes in 16 metabolic pathways (Fig. 9B). The analysis revealed that 23 differential metabolites between the sensitive and non-sensitive groups before radiotherapy (RB-S versus RB-NS) were significantly associated with 5 pathways, including ABC

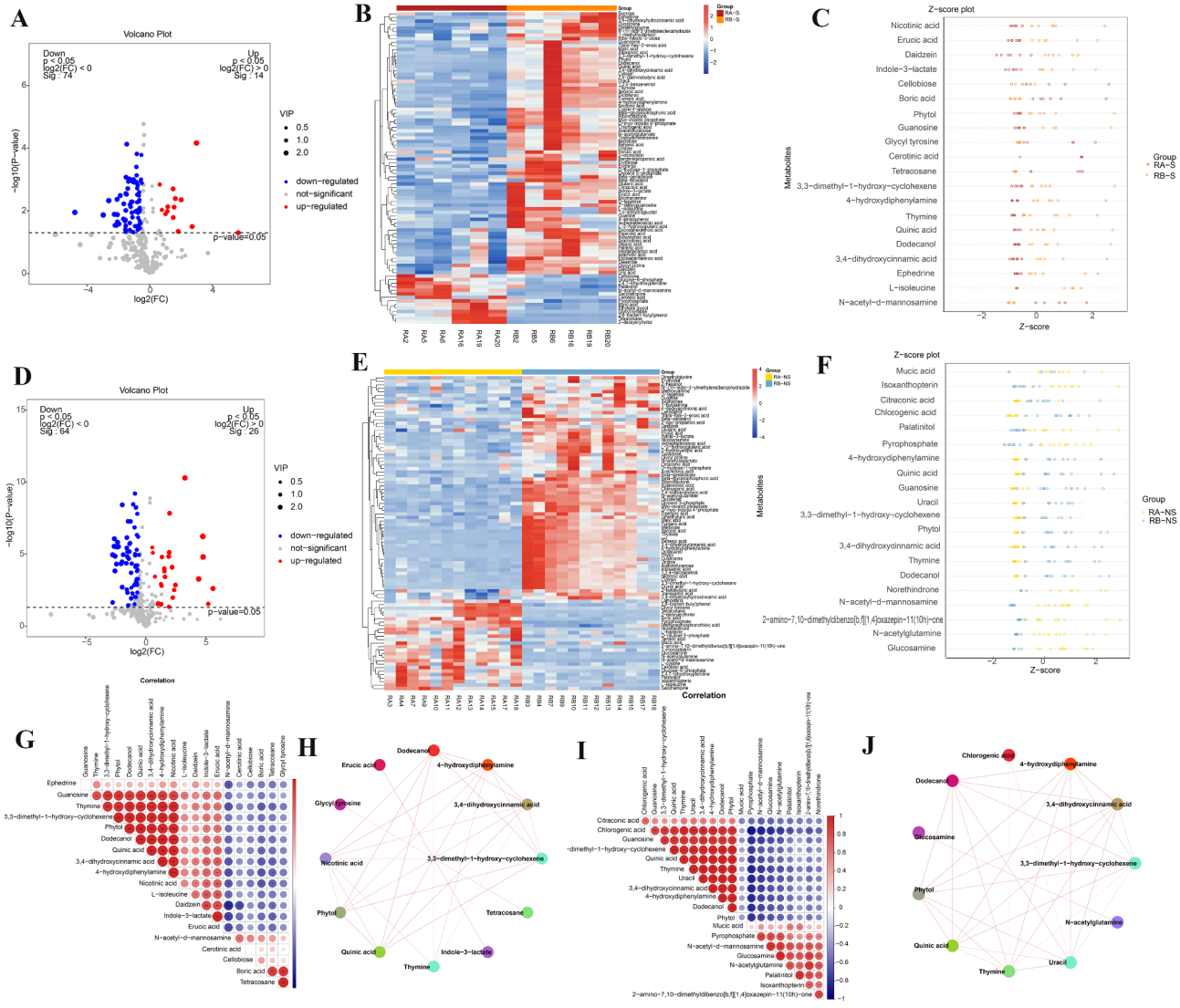

Fig. 7 Key metabolites in sensitive and non-sensitive groups before and after radiotherapy. **(A)** Volcano plot of key metabolites in sensitive groups before and after radiotherapy. **(B)** Heatmap of key metabolites in sensitive groups before and after radiotherapy. **(C)** Z-score plot of key metabolites in sensitive groups before and after radiotherapy. **(D)** Volcano plot of key metabolites in non-sensitive groups before and after radiotherapy. **(E)** Heatmap of key metabolites in non-sensitive groups before and after radiotherapy. **(F)** Z-score plot of key metabolites in non-sensitive groups before and after radiotherapy. **(G)** Correlation network of key metabolites in sensitive groups before and after radiotherapy. **(H)** Visualization of the correlation network for key metabolites in sensitive groups before and after radiotherapy. **(I)** Correlation network of key metabolites in non-sensitive groups before and after radiotherapy. **(J)** Visualization of the correlation network for key metabolites in non-sensitive groups before and after radiotherapy

transporters, taste transduction, protein digestion and absorption, shigellosis, and oxidative phosphorylation (Fig. 9C). After radiotherapy, seven differential metabolites between the sensitive and non-sensitive groups (RA-S versus RA-NS) were significantly related to 11 pathways, such as valine, leucine, and isoleucine biosynthesis, mineral absorption, central carbon metabolism in cancer, propanoate metabolism, valine, leucine, and isoleucine degradation, protein digestion and absorption, glycine, serine, and threonine metabolism, aminoacyl-tRNA biosynthesis, and cysteine and methionine metabolism (Fig. 9D). These pathways may represent the pivotal factors influencing the radiosensitivity of rectal cancer.

Predicting radiotherapy sensitivity based on serum metabolites

We subsequently employed random forests to identify key metabolites within patient groups exhibiting distinct sensitivities to radiotherapy, both before and after treatment. ROC curves were employed to evaluate the efficacy of individual metabolites or their combinations in predicting radiotherapy sensitivity. The relative

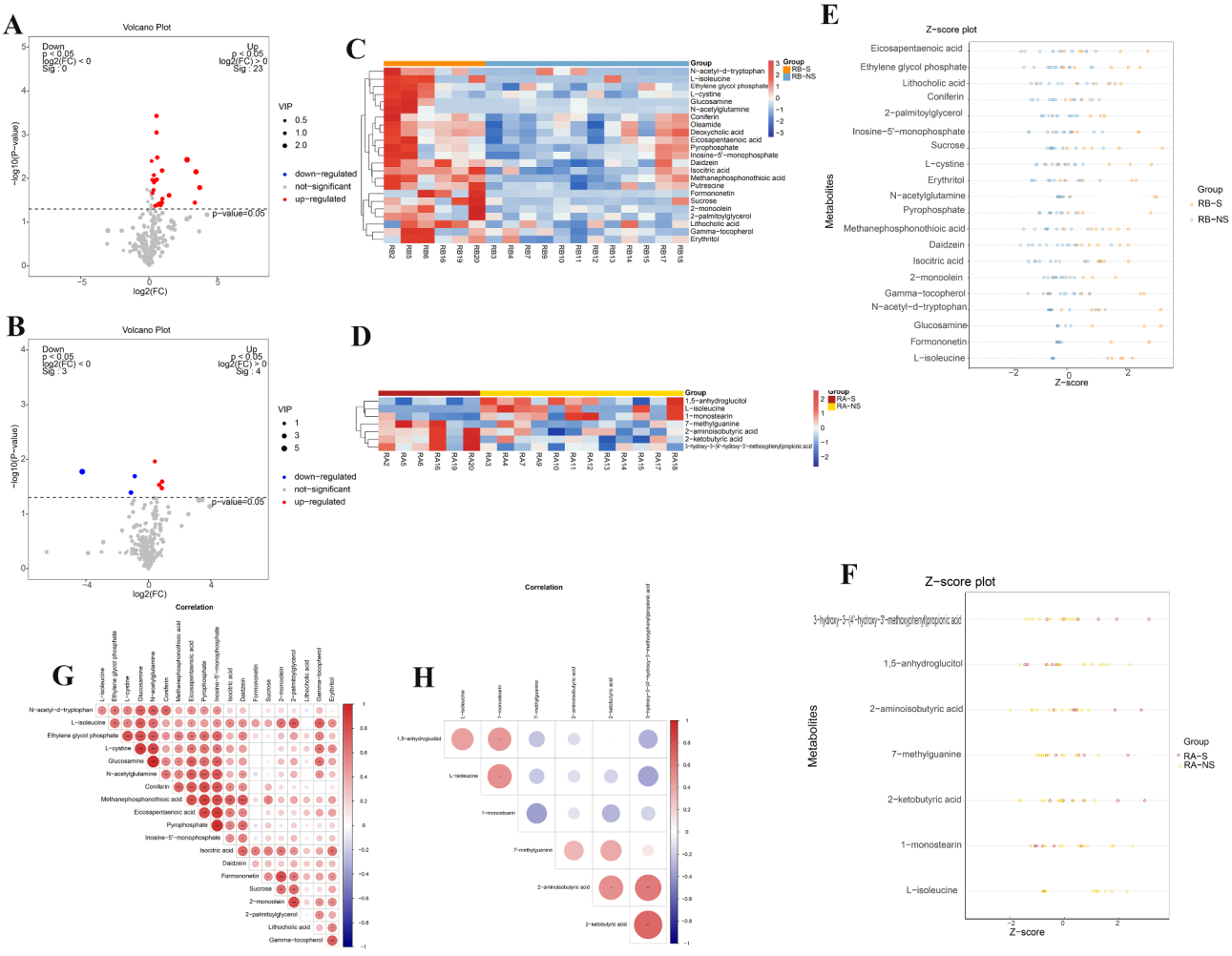

Fig. 8 Key metabolites distinguishing sensitive and non-sensitive groups before and after radiotherapy. **(A)** Volcano plot of key metabolites between sensitive and non-sensitive groups before radiotherapy. **(B)** Volcano plot of key metabolites between sensitive and non-sensitive groups after radiotherapy. **(C)** Heatmap of key metabolites between sensitive and non-sensitive groups before radiotherapy. **(D)** Heatmap of key metabolites between sensitive and non-sensitive groups after radiotherapy. **(E)** Z-score plot of key metabolites between sensitive and non-sensitive groups before radiotherapy. **(F)** Z-score plot of key metabolites between sensitive and non-sensitive groups after radiotherapy. **(G)** Correlation network of key metabolites between sensitive and non-sensitive groups before radiotherapy. **(H)** Correlation network of key metabolites between sensitive and non-sensitive groups after radiotherapy

abundance of significantly differentiating metabolites between the sensitive and non-sensitive groups, pre- and post-radiotherapy, is visualized in Figs. 10 and 11, respectively. The significance of these metabolites was assessed using Mean decrease accuracy and Mean decrease Gini (Fig. 12). As detailed in Table 2, three metabolites were identified as pivotal before radiotherapy: daidzein, isocitric acid, and 2-monoolein. These metabolites demonstrated strong predictive power for rectal cancer radiotherapy sensitivity, with isocitric acid exhibiting the highest predictive ability (AUC = 0.812). Furthermore, the combined impact of these three metabolites was even more pronounced (AUC = 0.875). Post-radiotherapy (Table 3), 3-hydroxy-3-(4'-hydroxy-3'-methoxyphenyl) propionic acid, L-isoleucine, 1-monostearin, 1,5-anhydroglucitol, 2-ketobutyric acid, 2-aminoisobutyric acid, and 7-methylguanine were identified as key metabolites. Among these, 3-hydroxy-3-(4'-hydroxy-3'-methoxyphenyl) propionic acid displayed the highest predictive capability (AUC = 0.75). Notably, the predictive accuracy was notably enhanced when combining multiple metabolites. These findings suggest that serum metabolites may serve as promising biomarkers for predicting rectal cancer radiotherapy sensitivity.

Discussion

Rectal cancer remains one of the most prevalent malignancies of the gastrointestinal tract, with its incidence steadily increasing worldwide. Radiotherapy is a cornerstone of rectal cancer treatment, significantly improving local control and survival outcomes. However, the heterogeneous response to radiotherapy among patients

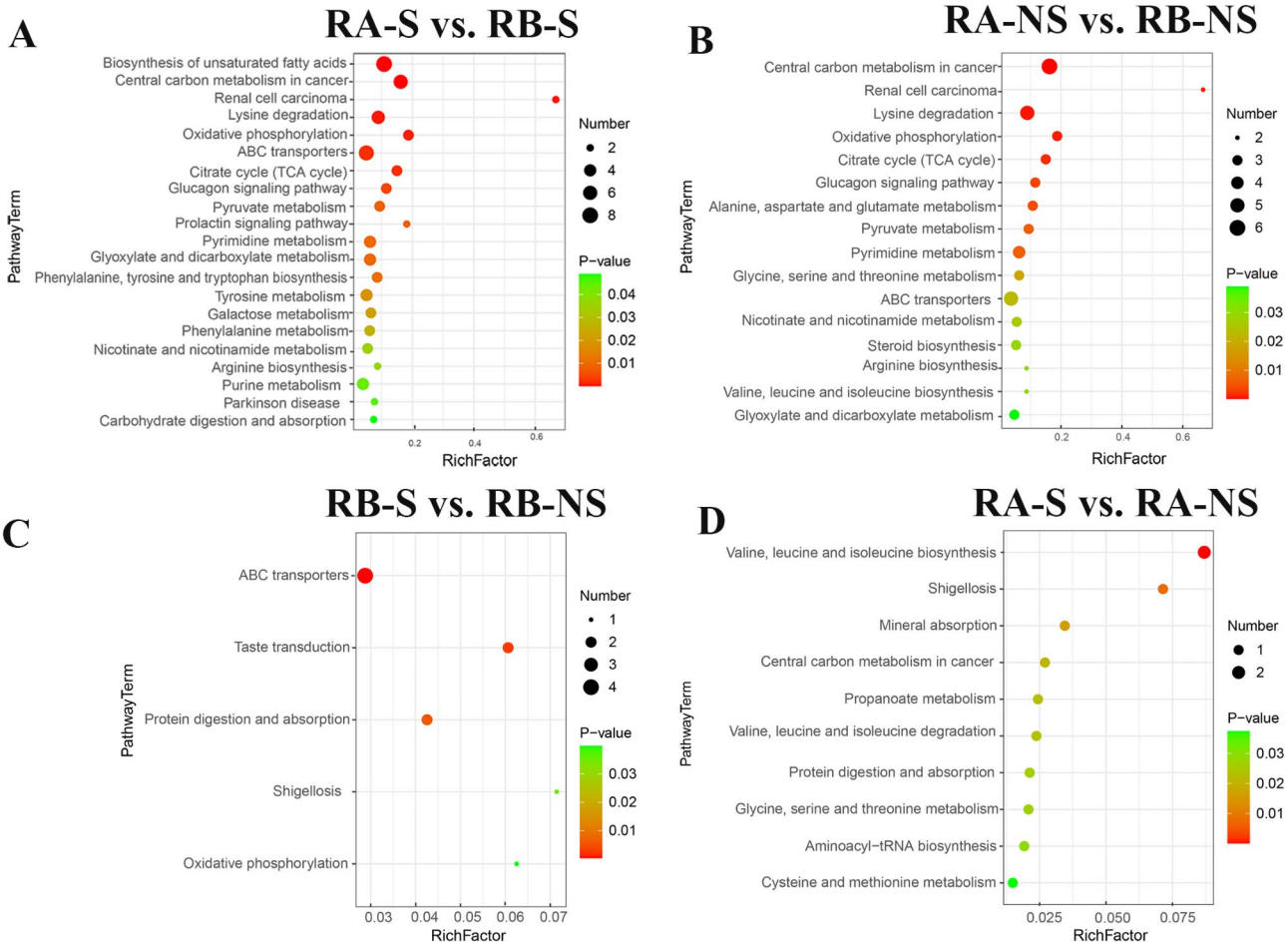

Fig. 9 Significantly enriched metabolic pathways in different sensitivity groups during NCRT. **(A)** Metabolic pathways enriched in RA-S vs. RB-S. **(B)** Metabolic pathways enriched in RA-NS vs. RB-NS. **(C)** Metabolic pathways enriched in RB-S vs. RB-NS. **(D)** Metabolic pathways enriched in RA-S vs. RA-NS

poses a significant challenge in predicting treatment efficacy. Recent advances in metabolomics have revealed a strong correlation between serum metabolites and tumor radiosensitivity, offering a novel approach to predicting treatment response and personalizing therapeutic strategies. Non-invasive biomarkers, particularly those derived from serum or other easily accessible biofluids, play a pivotal role in revolutionizing cancer diagnosis and treatment by enabling early detection, real-time monitoring of therapeutic response, and personalized treatment strategies, all while minimizing patient discomfort and procedural risks [26–28].

In this study, we explored the potential of serum metabolites as prognostic markers for radiotherapy response by analyzing metabolic profiles before, during, and after treatment. Our findings indicate that the serum metabolite profiles of rectal cancer patients undergo substantial transformations before, during, and after radiotherapy, which was consistent with previous studies [29]. This shift may be attributed to the impact of radiotherapy on the metabolic status of these patients. Radiotherapy disrupts DNA integrity and function in tumor cells, leading to cell death and the subsequent release of metabolites into the bloodstream. Consequently, these alterations in serum metabolites may serve as indicators of tumor cell damage and metabolic reprogramming.

In this study, we identified several key metabolites, including N-acetylglutamine, glucosamine, glycerol 3-phosphate, L-cystine, and arachidonic acid, that exhibited significant changes following radiotherapy. These metabolites are critically involved in the biological processes underlying radiation therapy. For example, arachidonic acid and its derivatives have been implicated in radiation response mechanisms, with studies suggesting that targeting enzymes involved in arachidonic acid metabolism could enhance radiotherapy efficacy [30]. Additionally, these metabolites are integral to several critical metabolic pathways that play essential roles during radiotherapy, such as lysine degradation, alanine-aspartate-glutamate metabolism, central carbon metabolism in cancer, oxidative phosphorylation, ferroptosis, pyrimidine metabolism, pyruvate metabolism,

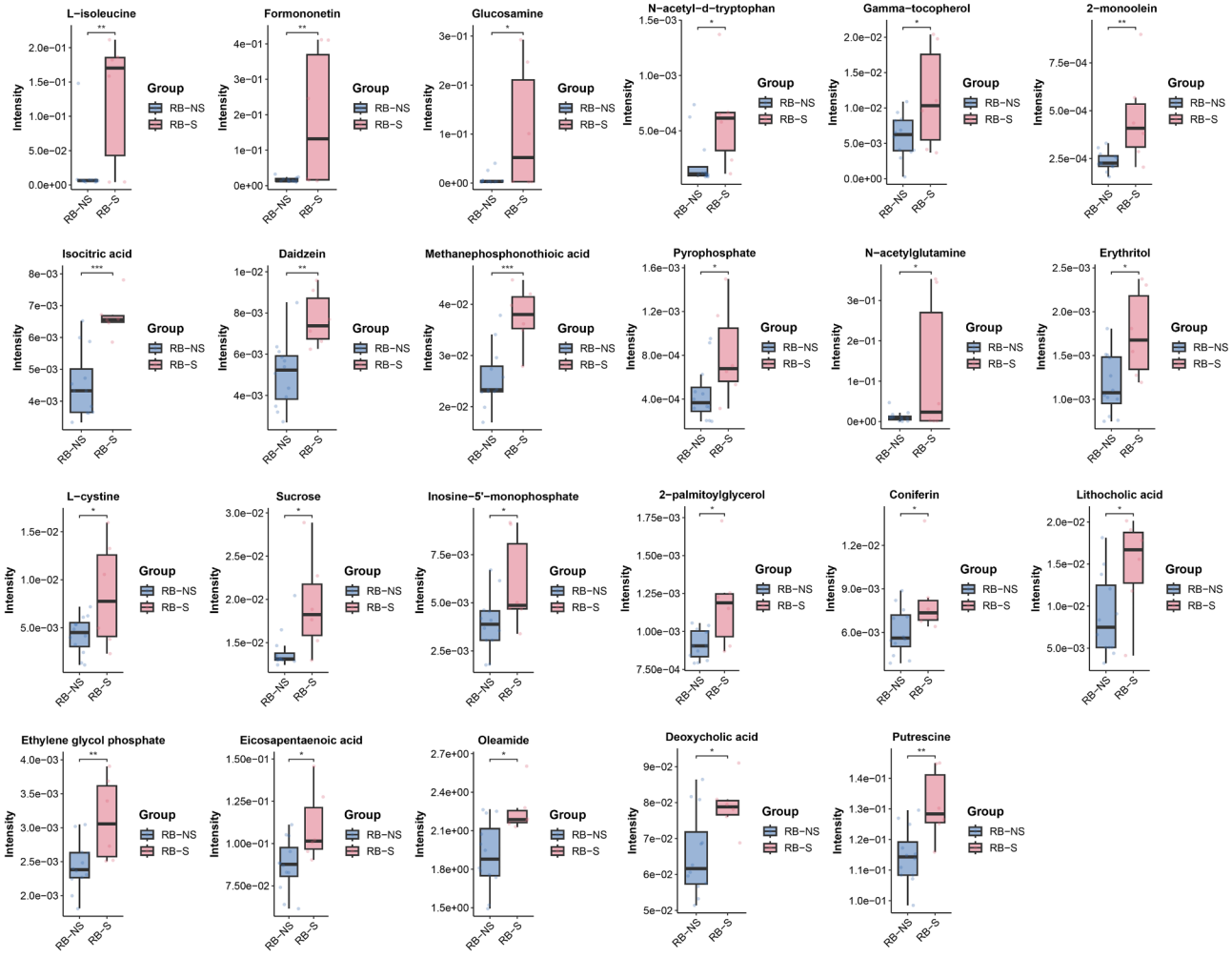

Fig. 10 Abundance of key metabolites in sensitive and non-sensitive groups before radiotherapy

and adipocyte lipolysis regulation. Among these, ferroptosis—a form of regulated cell death driven by iron-dependent lipid peroxidation—has garnered significant attention for its role in cancer therapy. Ferroptosis is triggered by cellular stress, radiation, and immunotherapy, and targeting this pathway has shown promise as a novel strategy to improve clinical outcomes in cancer treatment [31, 32]. These findings highlight the potential of modulating specific metabolic pathways to enhance the therapeutic effects of radiotherapy.

The observed changes in serum metabolites may reflect the radiosensitivity of rectal cancer patients. The underlying mechanism by which serum metabolites influence rectal cancer radiotherapy sensitivity may be multifaceted. Firstly, metabolites that interact with cells within the tumor microenvironment: these interactions can influence the radiotherapy sensitivity of tumor cells, and serum metabolites may modify this sensitivity by modulating these interactions. Secondly, metabolites involved in tumor cell signaling pathways: certain serum metabolites can function as signaling molecules within tumor cell signaling pathways, thereby affecting radiotherapy sensitivity. Thirdly, metabolites and tumor cell energy metabolism: tumor cells typically have heightened energy requirements, and radiotherapy can impact their growth by altering energy metabolism pathways. Serum metabolites may serve as byproducts of energy metabolism, reflecting the energy status of tumor cells and influencing radiotherapy sensitivity.

To further explore the predictive potential of serum metabolites, we compared metabolic profiles between radiotherapy-sensitive and -resistant patient groups before and after treatment. Our analysis revealed that certain metabolites were significantly reduced in the sensitive group, likely reflecting the direct cytotoxic effects of radiotherapy on tumor cells and the subsequent decline in metabolic activity. In contrast, these metabolites remained relatively stable in the resistant group, suggesting inherent or acquired mechanisms of radioresistance in these tumors. Among the differentially expressed

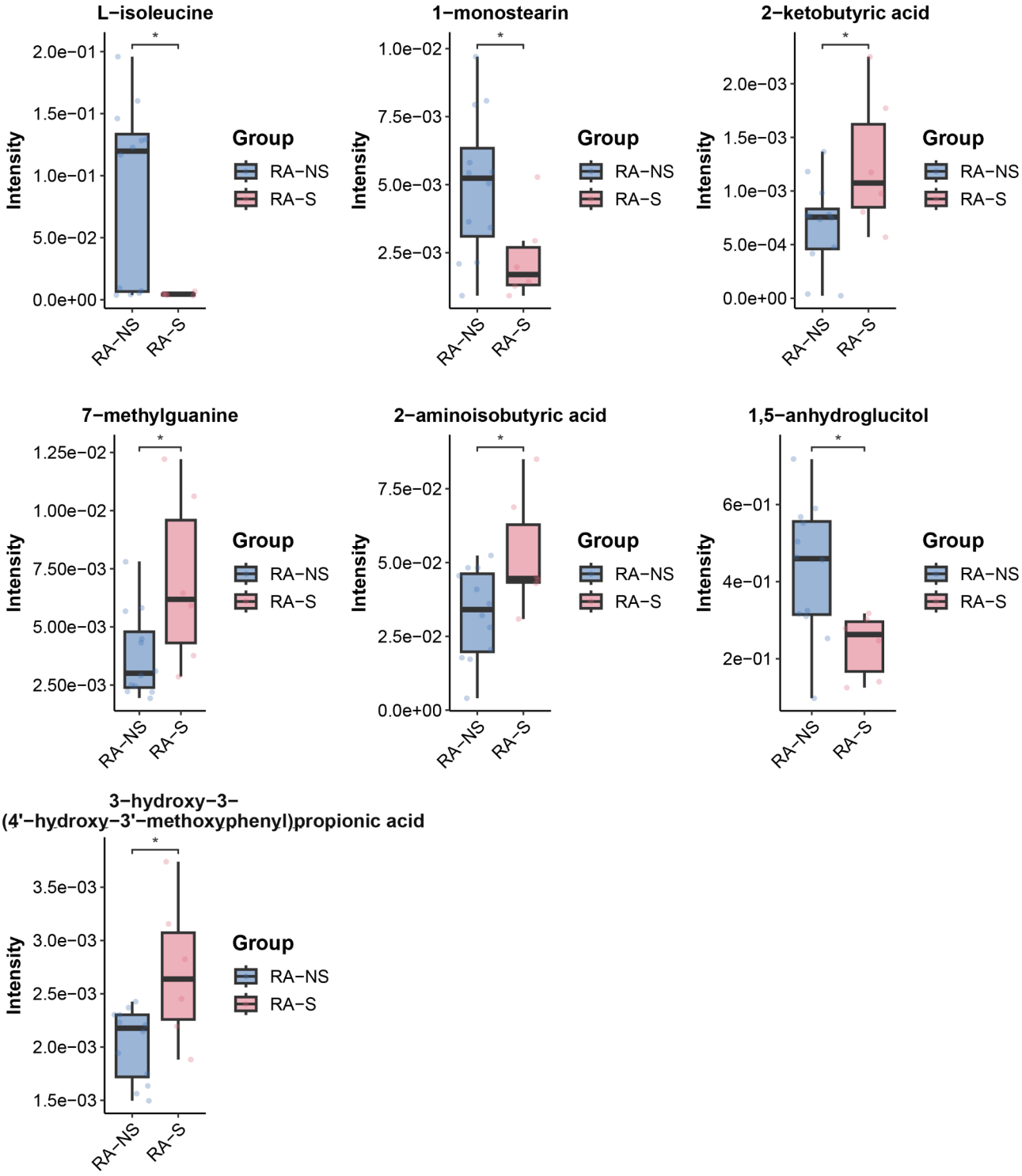

Fig. 11 Abundance of key metabolites in sensitive and non-sensitive groups after radiotherapy

metabolites, L-isoleucine emerged as a key candidate, showing significant variations between the sensitive and resistant groups both before and after radiotherapy. As an essential amino acid, L-isoleucine plays a critical role in numerous physiological processes, including protein synthesis and energy metabolism [33]. Recent studies have highlighted its potential influence on radiotherapy response, with evidence suggesting that L-isoleucine may modulate treatment efficacy through mechanisms such as regulating cell proliferation, enhancing DNA repair

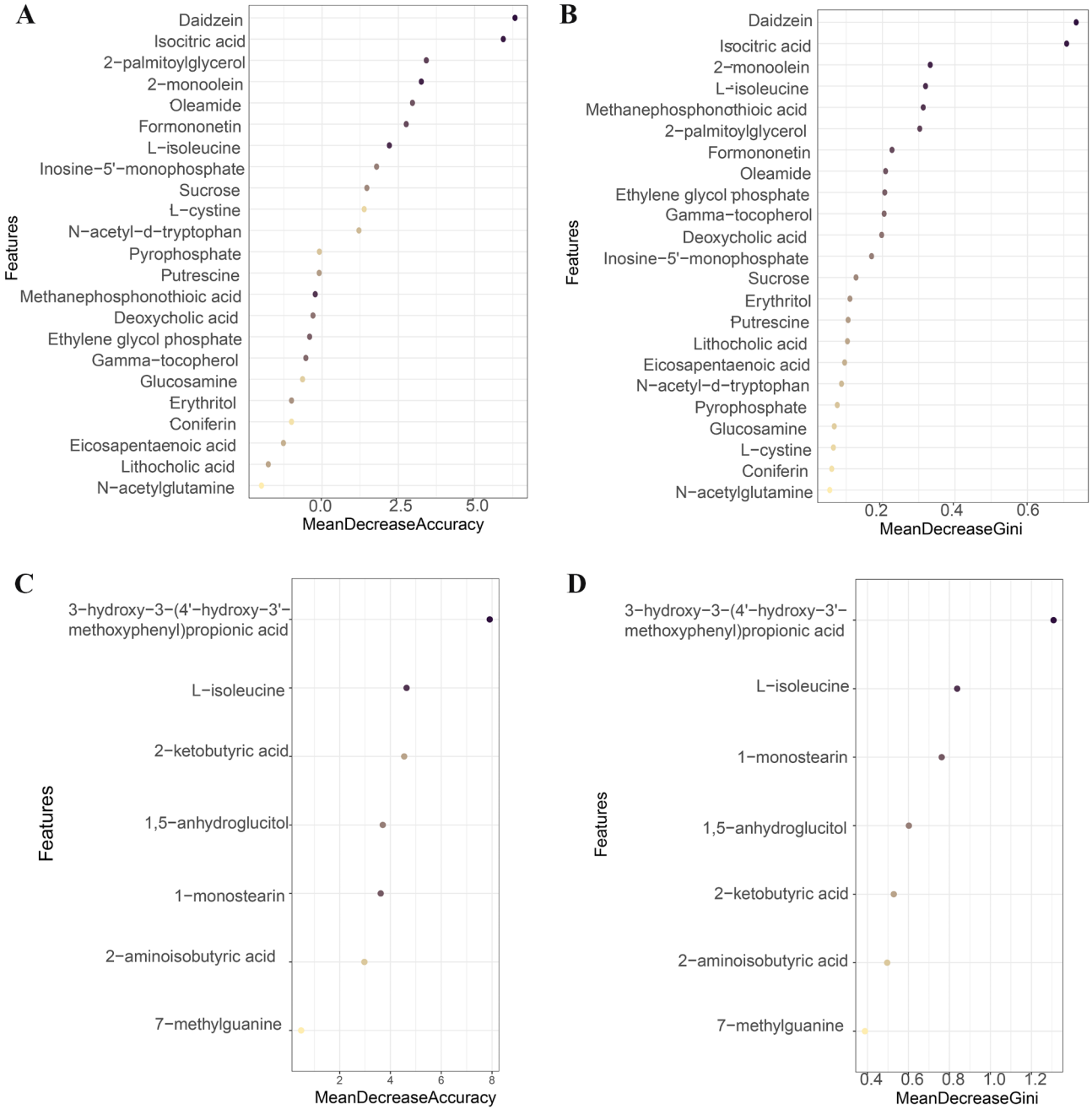

Fig. 12 Significance of key metabolites based on Mean Decrease Accuracy and Mean Decrease Gini. **(A)** Significance of key metabolites between sensitive and non-sensitive groups before radiotherapy, assessed by Mean Decrease Accuracy. **(B)** Significance of key metabolites between sensitive and non-sensitive groups before radiotherapy, assessed by Mean Decrease Gini. **(C)** Significance of key metabolites between sensitive and non-sensitive groups after radiotherapy, assessed by Mean Decrease Accuracy. **(D)** Significance of key metabolites between sensitive and non-sensitive groups after radiotherapy, assessed by Mean Decrease Gini

capacity, and influencing apoptotic pathways [34]. These findings underscore the potential of L-isoleucine and related metabolic pathways as biomarkers for predicting radiotherapy sensitivity and tailoring personalized treatment strategies.

In this study, we observed significant alterations in key metabolic pathways associated with radiotherapy sensitivity, both before and after treatment. Prior to radiotherapy, pathways such as ABC transporters, protein digestion and absorption, and oxidative phosphorylation were notably affected. Following radiotherapy, additional critical pathways were identified, including valine, leucine, and isoleucine biosynthesis and degradation, mineral absorption, central carbon metabolism in cancer,

Table 2 Pre-radiotherapy serum metabolites predict radiotherapy sensitivity in rectal cancer

Metabolite	AUC	Threshold	Sensitivity	Specificity	Accuracy
Daidzein	0.687	0.546	1	0.5	0.667
Isocitric acid	0.812	0.935	1	0.75	0.833
2-monoolein	0.687	0.327	0.5	1	0.833
Isocitric acid && Daidzein	0.812	0.617	1	0.75	0.833
2-monoolein && Isocitric acid && Daidzein	0.875	0.755	1	0.75	0.833

propanoate metabolism, glycine, serine, and threonine metabolism, aminoacyl-tRNA biosynthesis, and cysteine and methionine metabolism. These pathways are closely linked to cellular responses to radiation. For example, oxidative phosphorylation plays a dual role in radiation sensitivity. On one hand, it provides the energy required for essential cellular processes, such as DNA repair and apoptosis, which are critical for surviving radiation-induced damage. On the other hand, it generates reactive oxygen species (ROS) that exacerbate oxidative stress, leading to DNA and membrane lipid damage, thereby enhancing the cytotoxic effects of radiotherapy [35, 36]. Similarly, branched-chain amino acids (BCAAs) like valine, leucine, and isoleucine influence radiosensitivity by regulating intracellular redox balance and protecting cells from oxidative damage [37]. These findings underscore the complex interplay between metabolic pathways and radiation response, highlighting potential targets for improving therapeutic outcomes.

The radiosensitivity of rectal cancer is influenced by a complex interplay of factors, making it difficult to predict treatment outcomes using a single biomarker. Previous studies, including our own, have demonstrated that combining multiple biomarkers significantly improves accuracy in disease diagnosis, prognosis, and treatment planning compared to relying on individual markers [38–40]. Integrated metabolic profiling, in particular, provides a more comprehensive and precise representation of an organism's metabolic state, offering superior predictive power over isolated metabolites [41]. In this study, we employed a Random Forest-based machine learning approach to identify key serum metabolites associated with radiotherapy sensitivity or resistance in rectal cancer patients, both before and after treatment. We evaluated the predictive performance of individual metabolites as well as combined biomarker panels. Our results indicate that serum metabolites, especially when used in combination, hold significant promise as biomarkers for predicting radiotherapy sensitivity in rectal cancer patients. This approach not only enhances predictive accuracy but also provides a foundation for developing

Table 3 Post-radiotherapy serum metabolites predict radiosensitivity in rectal cancer

Metabolite	AUC	Threshold	Sensitivity	Specificity	Accuracy
3-hydroxy-3-(4′-hydroxy-3′-methoxyphenyl)propionic acid	0.75	0.999	1	0.5	0.667
L-isoleucine	0.5	0.255	1	0.25	0.5
L-isoleucine	0.5	0.669	0.5	0.75	0.667
1-monostearin	0.375	-	1	0	0.333
1-monostearin	0.375	-	0	1	0.667
1,5-anhydroglucitol	0.5	0.452	1	0.5	0.667
2-ketobutyric acid	0.5	0.858	0.5	0.75	0.667
2-aminoisobutyric acid	0.687	0.997	1	0.5	0.667
7-methylguanine	0.625	0.25	0.5	1	0.833
L-isoleucine && 3-hydroxy-3-(4′-hydroxy-3′-methoxyphenyl)propionic acid	0.625	0.846	1	0.5	0.667
L-isoleucine && 1-monostearin && 3-hydroxy-3-(4′-hydroxy-3′-methoxyphenyl) propionic acid	0.625	0.549	1	0.5	0.667
L-isoleucine && 1-monostearin && 1,5-anhydroglucitol && 3-hydroxy-3-(4′-hydroxy-3′-methoxyphenyl)propionic acid	0.875	0.579	1	0.5	0.667
L-isoleucine && 1-monostearin && 2-ketobutyric acid && 1,5-anhydroglucitol && 3-hydroxy-3-(4′-hydroxy-3′-methoxyphenyl)propionic acid	0.875	0.567	1	0.75	0.833
L-isoleucine && 1-monostearin && 2-ketobutyric acid && 2-aminoisobutyric acid && 1,5-anhydroglucitol && 3-hydroxy-3-(4′-hydroxy-3′-methoxyphenyl)propionic acid	0.875	0.625	1	0.75	0.833
L-isoleucine && 1-monostearin && 2-ketobutyric acid && 7-methylguanine && 2-aminoisobutyric acid && 1,5-anhydroglucitol && 3-hydroxy-3-(4′-hydroxy-3′-methoxyphenyl)propionic acid	0.75	0.707	1	0.75	0.833
L-isoleucine && 1-monostearin && 2-ketobutyric acid && 7-methylguanine && 2-aminoisobutyric acid && 1,5-anhydroglucitol && 3-hydroxy-3-(4′-hydroxy-3′-methoxyphenyl)propionic acid	0.75	0.504	1	0.5	0.667

personalized treatment strategies tailored to individual patient responses.

Serum metabolites that predict radiotherapy sensitivity in rectal cancer have significant potential to transform clinical practice [7, 9, 42]. First, the analysis of serum metabolites enables clinicians to more accurately predict radiotherapy efficacy, facilitating tailored treatment plans that optimize therapeutic outcomes. Second, the non-invasive nature of serum metabolite profiling enhances patient compliance and comfort, making it a practical tool for routine clinical use. Finally, integrating serum metabolite data with other molecular biomarkers, such as genomic or proteomic markers, offers a comprehensive approach to personalized medicine, allowing for more precise and individualized treatment strategies for rectal cancer patients.

This study was not without its limitations. Firstly, the sample size was relatively modest with only one sample in each group, necessitating further expansion to validate the robustness of the findings. Secondly, the examination of serum metabolite alterations before and after radiotherapy did not account for other potential factors that could influence radiotherapy sensitivity. While the advancements in metabolomics technology have enabled the detection of a wide array of metabolites, the subsequent data processing and interpretation remain intricate tasks. Moreover, the establishment of standardized protocols and methods for assessing serum metabolite levels is essential to ensure the consistency and reproducibility of the results. In future investigations, a more comprehensive approach that integrates clinical data and additional biomarkers is warranted to enhance the precision and reliability of the predictive models. Due to the relatively small sample size and the short follow-up period in this initial phase of the study, we did not have sufficient data to perform a robust survival curve analysis. Survival analysis typically requires a larger cohort and longer follow-up to draw meaningful conclusions about the relationship between metabolites and patient outcomes.

This study was designed as a pilot investigation to explore potential metabolic changes and identify candidate biomarkers during NCRT in patients with LARC. The primary goal was to generate hypotheses and identify promising metabolites for further validation in larger cohorts. Despite the small sample size, we employed rigorous analytical methods, including GC-MS, to ensure the accuracy and reliability of the metabolomic data. The significant changes observed in metabolic profiles and pathways were statistically validated, and the identified biomarkers showed promising predictive power (e.g., AUC values of 0.875 and 0.75 for specific metabolites). Our findings are consistent with previous studies highlighting the role of metabolic alterations in cancer therapy response, which supports the biological plausibility of our results. In future studies, we plan to expand our cohort size, incorporate multi-omics data, and validate the identified serum metabolites in larger, independent patient populations to enhance the robustness and clinical applicability of our findings, while also exploring the integration of non-invasive biomarkers with other molecular and clinical parameters for more precise prediction of radiotherapy response in rectal cancer.

Conclusions

In conclusion, our study highlights the potential of serum metabolites as predictive biomarkers for radiotherapy response in rectal cancer. By elucidating the metabolic changes associated with radiation sensitivity, we provide a foundation for developing personalized treatment strategies that could improve patient outcomes. Further research is needed to validate these findings and explore their clinical applicability.

Abbreviations

LARC	Locally Advanced Rectal Cancer
NCRT	Neoadjuvant Chemoradiotherapy
GC-MS	Liquid Chromatography-Mass Spectrometry
TRG	Tumor Regression Grading
RB	Before Radiotherapy
RD	During Radiotherapy
RA	After Radiotherapy
PCA	Principal Component Analysis
PLS-DA	Partial Least Squares Analysis
OPLS-DA	Orthogonal Partial Least Squares Analysis
VIP	Variable Important In Projection

Acknowledgements

Not applicable.

Author contributions

QP, YS (Yi Shen), and YX (Yingying Xu) performed the computational analysis, and wrote the manuscript. ZF, YX (Yao Xu), YW and LZ took part in the data analysis. YZ, and YS (Yuntian Shen) conceived of the study, and took part in its design and coordination. All authors read and approved the final manuscript.

Funding

This work was supported by National Natural Science Foundation of China grants (82003219), Scientific Research Program for Young Talents of China National Nuclear Corporation, Suzhou Science and Education Project (KJXW2023091), Suzhou Radiotherapy Clinical Medical Center (Szlcyxzx202103), Gusu Health Talent Research Program (GSWS2023043), Young Talent Support Project of the Second Affiliated Hospital of Soochow University (XKTJ-RC202408), Nuclear Technology Medical Application Program for Key Talents of the Second Affiliated Hospital of Soochow University (XKTJ-HRC20210013), the Second Affiliated Hospital of Soochow university pre-research project funding (SDFEYHT2225), and Project of State Key Laboratory of Radiation Medicine and Protection, Soochow University (GZK12023016, GZK12023029).

Data availability

No datasets were generated or analysed during the current study.

Declarations

Ethical approval and consent to participate

This study was reviewed and approved by the Ethics Committee of the Second Affiliated Hospital of Soochow University and was conducted under the Declaration of Helsinki ethical principles for medical research involving human subjects. Informed consent was obtained from the children's parents.

All participants provided both written and verbal consent to be part of this study.

Consent to publish
Not applicable.

Competing interests
The authors declare no competing interests.

Author details
[1]Department of Radiotherapy & Oncology, The Second Affiliated Hospital of Soochow University, San Xiang Road No. 1055, Suzhou, Jiangsu 215004, China
[2]Institute of Radiotherapy & Oncology, Soochow University, Suzhou, China
[3]State Key Laboratory of Radiation Medicine and Protection, Soochow University, Suzhou, China
[4]Department of Radiation Oncology, Suzhou Research Center of Medical School, Suzhou Hospital, Affiliated Hospital of Medical School, Nanjing University, Suzhou, China
[5]Department of Oncology, The Second Affiliated Hospital of Soochow University, Suzhou, China
[6]Department of Radiology, The Second Affiliated Hospital of Soochow University, Suzhou, China

Received: 8 November 2024 / Accepted: 25 February 2025
Published online: 12 March 2025

References

1. Siegel RL, Wagle NS, Cercek A, Smith RA, Jemal A. Colorectal cancer statistics, 2023. CA Cancer J Clin. 2023;73(3):233–54.
2. Schrag D, Shi Q, Weiser MR, Gollub MJ, Saltz LB, Musher BL, et al. Preoperative treatment of locally advanced rectal Cancer. N Engl J Med. 2023;389(4):322–34.
3. Jin J, Tang Y, Hu C, Jiang LM, Jiang J, Li N, et al. Multicenter, randomized, phase III trial of Short-Term radiotherapy plus chemotherapy versus Long-Term chemoradiotherapy in locally advanced rectal Cancer (STELLAR). J Clin Oncol. 2022;40(15):1681–92.
4. Pham TT, Lim S, Lin M. Predicting neoadjuvant chemoradiotherapy response with functional imaging and liquid biomarkers in locally advanced rectal cancer. Expert Rev Anticancer Ther. 2022;22(10):1081–98.
5. Schmidt DR, Patel R, Kirsch DG, Lewis CA, Vander Heiden MG, Locasale JW. Metabolomics in cancer research and emerging applications in clinical oncology. CA Cancer J Clin. 2021;71(4):333–58.
6. Anwardeen NR, Diboun I, Mokrab Y, Althani AA, Elrayess MA. Statistical methods and resources for biomarker discovery using metabolomics. BMC Bioinformatics. 2023;24(1):250.
7. Lv J, Jia H, Mo M, Yuan J, Wu Z, Zhang S, et al. Changes of serum metabolites levels during neoadjuvant chemoradiation and prediction of the pathological response in locally advanced rectal cancer. Metabolomics. 2022;18(12):99.
8. Jia H, Shen X, Guan Y, Xu M, Tu J, Mo M, et al. Predicting the pathological response to neoadjuvant chemoradiation using untargeted metabolomics in locally advanced rectal cancer. Radiother Oncol. 2018;128(3):548–56.
9. Wang H, Jia H, Gao Y, Zhang H, Fan J, Zhang L, et al. Serum metabolic traits reveal therapeutic toxicities and responses of neoadjuvant chemoradiotherapy in patients with rectal cancer. Nat Commun. 2022;13(1):7802.
10. Beale DJ, Pinu FR, Kouremenos KA, Poojary MM, Narayana VK, Boughton BA, et al. Review of recent developments in GC-MS approaches to metabolomics-based research. Metabolomics. 2018;14(11):152.
11. Lubes G, Goodarzi M. GC-MS based metabolomics used for the identification of cancer volatile organic compounds as biomarkers. J Pharm Biomed Anal. 2018;147:313–22.
12. Kiseleva O, Kurbatov I, Ilgisonis E, Poverennaya E. Defining blood plasma and serum metabolome by GC-MS. Metabolites 2021;12(1).
13. Ueta I, Sumiya K, Fujimura K, Ariizumi Y, Kikuchi R, Kawata K et al. Volatile anticancer drug determination by thermal desorption technique with polydimethylsiloxane-coated macroporous silica adsorbent in gas chromatography-mass spectrometry. Anal Sci 2023.
14. Zhu J, Liu A, Sun X, Liu L, Zhu Y, Zhang T, et al. Multicenter, randomized, phase III trial of neoadjuvant chemoradiation with capecitabine and Irinotecan guided by UGT1A1 status in patients with locally advanced rectal Cancer. J Clin Oncol. 2020;38(36):4231–9.
15. Chen HY, Feng LL, Li M, Ju HQ, Ding Y, Lan M, et al. College of American pathologists tumor regression grading system for Long-Term outcome in patients with locally advanced rectal Cancer. Oncologist. 2021;26(5):e780–93.
16. Tsugawa H, Cajka T, Kind T, Ma Y, Higgins B, Ikeda K, et al. MS-DIAL: data-independent MS/MS Deconvolution for comprehensive metabolome analysis. Nat Methods. 2015;12(6):523–6.
17. Choquette SJ, Duewer DL, Sharpless KE. NIST reference materials: utility and future. Annu Rev Anal Chem (Palo Alto Calif). 2020;13(1):453–74.
18. Alonso A, Marsal S, Julia A. Analytical methods in untargeted metabolomics: state of the Art in 2015. Front Bioeng Biotechnol. 2015;3:23.
19. Chen B, Wang Y, Wang Q, Li D, Huang X, Kuang X, et al. Untargeted metabolomics identifies potential serum biomarkers associated with Crohn's disease. Clin Exp Med. 2023;23(5):1751–61.
20. Boccard J, Rutledge DN. A consensus orthogonal partial least squares discriminant analysis (OPLS-DA) strategy for multiblock omics data fusion. Anal Chim Acta. 2013;769:30–9.
21. Kumar L. Mfuzz: a software package for soft clustering of microarray data. Bioinformation. 2007;2(1):5–7.
22. Kanehisa M, Furumichi M, Sato Y, Ishiguro-Watanabe M, Tanabe M. KEGG: integrating viruses and cellular organisms. Nucleic Acids Res. 2021;49(D1):D545–51.
23. Basith S, Manavalan B, Hwan Shin T, Lee G. Machine intelligence in peptide therapeutics: A next-generation tool for rapid disease screening. Med Res Rev. 2020;40(4):1276–314.
24. Hajian-Tilaki K. Receiver operating characteristic (ROC) curve analysis for medical diagnostic test evaluation. Casp J Intern Med. 2013;4(2):627–35.
25. Wang H, Yang F, Luo Z. An experimental study of the intrinsic stability of random forest variable importance measures. BMC Bioinformatics. 2016;17:60.
26. Jing Y, Huang X, Wang Y, Wang J, Li Y, Yelihamu D, et al. Diagnostic value of 5 MiRNAs combined detection for breast cancer. Front Genet. 2024;15:1482927.
27. Luo Z, Wang Y, Bi X, Ismtula D, Wang H, Guo C. Cytokine-induced apoptosis inhibitor 1: a comprehensive analysis of potential diagnostic, prognosis, and immune biomarkers in invasive breast cancer. Transl Cancer Res. 2023;12(7):1765–86.
28. Peng Q, Tao J, Xu Y, Shen Y, Wang Y, Jiao Y, et al. Lipid metabolism-associated genes serve as potential predictive biomarkers in neoadjuvant chemoradiotherapy combined with immunotherapy in rectal cancer. Transl Oncol. 2024;39:101828.
29. Peng Q, Jiang L, Shen Y, Xu Y, Shen X, Zou L, et al. LC-MS metabolomics analysis of serum metabolites during neoadjuvant chemoradiotherapy in locally advanced rectal cancer. Clin Transl Oncol. 2024;26(12):3150–68.
30. Kim W, Son B, Lee S, Do H, Youn B. Targeting the enzymes involved in arachidonic acid metabolism to improve radiotherapy. Cancer Metastasis Rev. 2018;37(2–3):213–25.
31. Chen X, Zhang L, He Y, Huang S, Chen S, Zhao W, et al. Regulation of m(6)A modification on ferroptosis and its potential significance in radiosensitization. Cell Death Discov. 2023;9(1):343.
32. Zheng X, Jin X, Ye F, Liu X, Yu B, Li Z, et al. Ferroptosis: a novel regulated cell death participating in cellular stress response, radiotherapy, and immunotherapy. Exp Hematol Oncol. 2023;12(1):65.
33. Liang YF, Long ZX, Zhang YJ, Luo CY, Yan LT, Gao WY, et al. The chemical mechanisms of the enzymes in the branched-chain amino acids biosynthetic pathway and their applications. Biochimie. 2021;184:72–87.
34. Peng H, Wang Y, Luo W. Multifaceted role of branched-chain amino acid metabolism in cancer. Oncogene. 2020;39(44):6747–56.
35. Boreel DF, Span PN, Heskamp S, Adema GJ, Bussink J. Targeting oxidative phosphorylation to increase the efficacy of Radio- and Immune-Combination therapy. Clin Cancer Res. 2021;27(11):2970–8.
36. Chen D, Barsoumian HB, Fischer G, Yang L, Verma V, Younes AI et al. Combination treatment with radiotherapy and a novel oxidative phosphorylation inhibitor overcomes PD-1 resistance and enhances antitumor immunity. J Immunother Cancer 2020;8(1).
37. Wu S, Liu X, Cheng L, Wang D, Qin G, Zhang X, et al. Protective mechanism of leucine and isoleucine against H(2)O(2)-Induced oxidative damage in bovine mammary epithelial cells. Oxid Med Cell Longev. 2022;2022:4013575.
38. Peng Q, Zhang X, Min M, Zou L, Shen P, Zhu Y. The clinical role of microRNA-21 as a promising biomarker in the diagnosis and prognosis of colorectal cancer: a systematic review and meta-analysis. Oncotarget. 2017;8(27):44893–909.

39. Peng Q, Shen Y, Lin K, Zou L, Shen Y, Zhu Y. Comprehensive and integrative analysis identifies microRNA-106 as a novel non-invasive biomarker for detection of gastric cancer. J Transl Med. 2018;16(1):127.
40. Peng Q, Feng Z, Shen Y, Zhu J, Zou L, Shen Y, et al. Integrated analyses of microRNA-29 family and the related combination biomarkers demonstrate their widespread influence on risk, recurrence, metastasis and survival outcome in colorectal cancer. Cancer Cell Int. 2019;19:181.
41. Peng Q, Zhan C, Shen Y, Xu Y, Ren B, Feng Z, et al. Blood lipid metabolic biomarkers are emerging as significant prognostic indicators for survival in cancer patients. BMC Cancer. 2024;24(1):1549.
42. Zhou H, Chen Y, Xiao Y, Wu Q, Li H, Li Y, et al. Evaluation of the ability of fatty acid metabolism signature to predict response to neoadjuvant chemoradiotherapy and prognosis of patients with locally advanced rectal cancer. Front Immunol. 2022;13:1050721.

Publisher's note